

# On the spectral hardening at $\sim > 300$ keV in solar flares

G. Li<sup>1,\*</sup>, X. Kong<sup>2,1</sup>, G. Zank<sup>1</sup>, Y. Chen<sup>2</sup>

<sup>1</sup> Department of Physics and CSPAR, University of Alabama in Huntsville, Huntsville, AL  
35899, USA

<sup>2</sup> Institute of Space Sciences and School of Space Sciences and Physics, Shandong  
University, Weihai, China, 264209

\* gang.li@uah.edu

Received \_\_\_\_\_; accepted \_\_\_\_\_

# ABSTRACT

It has been noted for a long time that the spectra of observed continuum emissions in many solar flares are consistent with double power laws with a hardening at energies  $\sim > 300$  keV. It is now largely believed that at least in electron-dominated events the hardening in photon spectrum reflects an intrinsic hardening in the source electron spectrum. In this paper, we point out that a power law spectrum of electron with a hardening at high energies can be explained by diffusive shock acceleration of electrons at a termination shock with a finite width. Our suggestion is based on an early analytical work by Drury et al., where the steady state transport equation at a shock with a tanh profile was solved for a  $p$ -independent diffusion coefficient. Numerical simulations with a  $p$ -dependent diffusion coefficient show hardenings in the accelerated electron spectrum which are comparable with observations. One necessary condition for our proposed scenario to work is that high energy electrons resonate with the inertial range of the MHD turbulence and low energy electrons resonate with the dissipation range of the MHD turbulence at the acceleration site, and the spectrum of the dissipation range  $\sim k^{-2.7}$ . A  $\sim k^{-2.7}$  dissipation range spectrum is consistent with recent solar wind observations.

*Subject headings:* Sun: flares — Sun: particle emission — Sun: X-rays, gamma rays  
— acceleration of particles

## 1. Introduction

Our Sun is an efficient particle accelerator. Ions with energy up to  $\sim GeV$ /nucleon are detected in-situ during large Solar Energetic Particle (SEP) events where both large flares and fast CMEs often occur together. At flares, electron Bremsstrahlung is believed to be the main source of the continuum radiation (e. g. Ramaty et al. (1975); Vestrand (1988)).

Continuum emissions provide invaluable information that constrains the underlying acceleration mechanism. These constraints include the energy budget, the total number of electrons, the acceleration time scales, etc. See reviews by Miller et al. (1997) and Zharkova et al. (2011) for a detail discussion on various acceleration mechanisms and the implications of these constraints on them.

One observational constraint that received less attention, even though has been noted for a long time, is the hardening of the continuum spectrum at high energies (often  $\sim > 300$  keV). In 1975, Suri et al. (1975) examined the X-ray and gamma-ray flux in the August 4, 1972 event and concluded that the X and gamma-ray flux was produced by a single population of electrons with a break in its spectrum, instead of two separate populations acting independently. Later, Yoshimori et al. (1985), using Hinotori spacecraft, examined the hard X-ray (HXR) spectrum in a broad energy range (20 keV - 7 MeV) for four flares that showed significant hardening at energies above  $\sim 400$  keV. They confirmed the earlier suggestion of Suri et al. (1975) that the hardening in the continuum reflects an underlying hardening in the source electron spectrum. Spectral hardening also occurs in events where there are clear signatures of gamma-ray lines. The most recent report of such an event is from the Fermi observation (see Ackermann et al. (2012)) where spectral hardening was found at above several hundred keV.

Note that hardening in the source electron spectrum is not the only cause for a hardening in the photon spectrum. Various processes, such as electron-electron

Bremsstrahlung, proton Bremsstrahlung, positronium annihilation continuum and inverse Compton emissions (see Vestrand (1988)), may all lead to some hardening of a continuum emission from a straight power law (without hardening) source electron spectrum. However, for parameters appropriate to a solar flare site, the contributions of these processes are relatively small and the resulting hardening of the spectral index is perhaps  $\sim 0.5$  (Kontar et al. 2007). Therefore these processes can not explain events where the change of spectral indices are as high as 2. Park et al. (1997) studied photon spectral hardening around 1 MeV for four flares. In their scenario, the emission is a simple sum of the thin target emission from the trapped electrons at the acceleration site near the loop top and the thick target emission from the escaping electrons precipitating on the solar surface. With the assumption that electrons having smaller energies have shorter escape times, and noted that the energy dependence of the Bremsstrahlung cross section differs in the nonrelativistic and the relativistic regimes, Park et al. (1997) were able to account for the observed spectral hardening. Note in the scenario of Park et al. (1997), the energy dependence of the escaping time decides the hardening, and the accelerated electron spectrum in the accelerated region does not (need to) have a spectral hardening. In-situ observations by Moses et al. (1989), however, showed that electron spectral hardening is rather common in short duration events. Assuming these in-situ electrons are the source electrons escaping from the acceleration site through interchange reconnection, then Moses et al. (1989)’s results also suggest that the accelerated electron population has a hardening at high energies.

High energy electrons also lead to microwave emissions through gyro-synchrotron radiation (see e.g. the recent review by White et al. (2011) for a detailed discussion of the relationship between solar radio and HXR emissions). In an early study, using BATSE (HXRs) and Owens Valley Radio Observatory (microwaves), Silva et al. (2000) examined 27 solar flares with multiple peaks (a total of 57) which were observed at both HXR and microwave wavelengths. Fitting the HXR spectra by a single power law and the microwave

spectra as gyrosynchrotron emissions, Silva et al. (2000) found that in 75% of the bursts, the inferred spectral indices of the electron energy distribution of the microwave-emitting electrons were harder (by 0.5 to 2.0) than those of the lower energy HXR emitting electrons. Silva et al. (2000) concluded that there exists a breakup in the energy spectra of the source electrons at around  $\sim 300$  keV, in agreement with previous observations of HXR-alone spectra of giant flares.

Note, however, in most events the HXRs are emanated from the footpoints of flare loops and microwaves are emanated from the tops of flare loops. Furthermore, there is also a delay between the peak of the microwave emission and the HXR emission. So there are transport effects between electrons generating microwave emissions and those generating HXRs White et al. (2011). Both the harder HXR spectrum at the footpoints and the delays of the microwave emission could be caused by magnetic trapping of higher energy electrons near the looptop and the precipitation of lower energy electron to the footpoints, as first suggested by Melrose and Brown (1976). In a recent study by Kawate et al. (2012), HXR and microwave emissions from 10 flares were analyzed. Although the emissions were at different locations and the spectral indices for microwave emissions are harder than those of the HXRs, by assuming a spectrum for the accelerated electrons that is consistent with the HXR emissions (but extend to higher energies), Kawate et al. (2012) were able to produce microwave spectra comparable to the observations. The authors concluded that it is a single electron population that is responsible for the HXRs and microwaves emissions and the hardening of the microwave emission is due to a more efficient trapping of electrons with higher energies. In another study, to minimize the effect of the trapping of high energy electrons on the resulting spectra of looptop microwave emissions, Asai et al. (2013) examined both the HXR and microwave spectra prior to the peak emission in 12 flares. They still find a significant hardening of the source electrons for the microwave emissions. These authors suggest that there is an intrinsic spectral hardening for the source electron

spectrum around several hundreds of keV and the microwave gyrosynchrotron emission is due to electrons at higher energies (in the harder part of the spectrum).

In this work, we do not consider microwave emissions and focus on HXR alone. Vestrand et al. (1999) identified 258 flare events using SMM observations. Among these, many are electron-dominated events with no clear signature of gamma-ray emissions (Rieger & Marschhauser 1990; Marschhauser et al. 1994). In these events, the contribution of nuclear gamma ray lines is minimal and the continuum is mainly due to Bremsstrahlung of the energetic electrons. The spectral hardening can be clearly seen in many of those electron-dominate events. A careful examination of these events based on the mechanism proposed here will be reported elsewhere (Kong et al. to be submitted).

A hardening in the source electron spectra is hard to explain for any acceleration mechanism. In this paper, we propose a scenario which is based on diffusive shock acceleration (DSA) to explain the observed spectral hardening.

Electron acceleration at a termination shock (TS) in solar flares is not a new idea. Tsuneta & Naito (1998) were the first to consider electron acceleration via DSA at a flare TS. Tsuneta & Naito (1998) pointed out that slow shocks bounding the reconnection X-point can heat the plasma up to perhaps 10-20 MK, providing abundant seed population which are accelerated to 1 MeV in 0.3 to 0.6 seconds at the TS.

Noting that the standing TS is of quasi-perpendicular in nature, Mann et al. (2009) considered shock drift acceleration (SDA) at a standing TS. In the work of Mann et al. (2009), most energy gain of electrons is through a single reflection at the shock front. Therefore to accelerate electrons to high energies, a stringent requirement of  $\theta_{BN}$  (e.g.  $\theta_{BN} > 88^\circ$ ) is needed. However, while the TS on large scale is of quasi-perpendicular, small scale structures (such as ripples) exist on the shock front. Indeed, the plasma in the reconnection region is unlikely to be homogeneous, so the resulting TS is unlikely to be

planar. Recently, Guo & Giacalone (2012) have examined electron acceleration at a flare TS using a hybrid code. In the simulation of Guo & Giacalone (2012), many small scale ripples were identified along the shock surface. The existence of these ripples suggests that assuming a shock with a  $\theta_{BN} > 88^\circ$  across the shock surface may be unrealistic. Furthermore, the existence of these small scale structures implies that one single field line can intersect the shock surface multiple times. Consequently, the acceleration process will be of diffusive in nature. In this work, we follow Tsuneta & Naito (1998) and assume the electron acceleration at a flare shock can be described by the DSA mechanism. Note that the existence of a TS in a flare site is not trivial. Observational evidence of flare TS has been reported by Warmuth et al. (2009), who used dynamic radio spectrum from the Trensorf radiospectrograph to show that there was a type-II radio bursts from a standing TS at  $\sim 300$  MHz during the impulsive phase of the X1.7 flare of 2001 March 29. Besides the existence of a TS, the area of the TS shock has also to be large enough ( $\sim 10^{20}$  cm<sup>2</sup> in large flares ) to account for the observed flux of HXRs generated by high energy electrons. By assuming a 50% contour of the NRH source at 327 MHz (see Figure 2 of (Warmuth et al. 2009) ) being a proxy for the shock, Warmuth et al. (2009) estimated a shock area of  $\sim 1.3 \times 10^{20}$  cm<sup>2</sup> in the 2001 March 29 X1.7 flare. We do note that these areas are much larger than the areas of HXR sources and are more comparable to active region sizes. Whether or not the size of the TS can be this large remains to be examined. Using the same technique, Warmuth et al. (2009) nevertheless obtained similar areas for other events where TS were observed. Of course, for smaller flares (like M flares), the area of the active region is smaller and we expect the area of the shock is also smaller.

Besides shock acceleration, models based on stochastic (aka 2nd-order Fermi) acceleration exist. For example, Miller et al. (1996, 1997) assumed the presence of some large scale turbulence at the flare site and considered the coupled system of the wave cascading and particle acceleration. Miller et al. (1996, 1997) showed that various modes

of waves (Alfvénic and fast mode waves), as they cascade to small scales, can efficiently accelerate both ions and electrons. Similar processes have also been studied by, for example, Petrosian et al. (1994); Park et al. (1997). Unlike Miller et al. (1996, 1997), Petrosian et al. (1994); Park et al. (1997) did not address the cascading of the turbulence and assumed the wave spectra is given.

In this work, we do not consider stochastic acceleration. However, as in Petrosian et al. (1994); Miller et al. (1996, 1997); Park et al. (1997), we assume the diffusion coefficient  $\kappa$  is decided by the underlying turbulence power at a flare site.

## 2. Diffusive shock acceleration of electrons at a finite-width termination shock

At a piecewise shock, the standard steady state DSA predicts a power law spectrum  $\sim p^{-\alpha}$  for energetic particles. The power law spectral index  $\alpha$  is given by  $3s/(s-1)$ , where  $s = u_1/u_2$  is the compression ratio,  $u_1$  and  $u_2$  the upstream and downstream flow speed in the shock frame. In the case of a shock having a finite width  $\sim L_{diff}$ , Drury et al. (1982) showed that the spectral index depends on the shock width. Assuming the background fluid speed is given by a tanh profile:

$$u(x) = \frac{u_1 + u_2}{2} - \frac{u_1 - u_2}{2} \tanh(x/L_{diff}) \quad (1)$$

then the spectral index  $\alpha$  becomes (Drury et al. 1982),

$$\alpha = \frac{3s}{s-1} \left( 1 + \frac{1}{\beta_s} \frac{1}{s-1} \right) \quad (2)$$

where  $\beta_s$  is a dimensionless parameter and is related to the diffusion coefficient  $\kappa$  through,

$$\kappa = \beta_s (u - u_1)(u - u_2) \frac{dx}{du} = \beta_s \frac{u_1 - u_2}{2} L_{diff}. \quad (3)$$

Although Drury et al. (1982) considered only the case of  $p$ -independent  $\kappa$  where analytical solutions can be obtained, one can see from the above that for a  $\kappa$  increasing with  $p$  the



spectrum will harden at high energies. Because the factor of  $1/\beta_s$  in equation (2), the spectral index quickly approaches the limit of  $3s/(s-1)$  when  $\beta_s \geq 1$ . When  $\beta_s$  is small, however, the second term in the bracket of equation (2) dominates and the spectrum can be very soft.

Clearly the momentum dependence of the diffusion coefficient  $\kappa$  decides the shape of the spectrum. At a flare site, the  $\kappa$  of energetic electrons is decided by the turbulence level. At large scales, the turbulence is of Alfvénic and particle-wave cyclotron resonance can accelerate ions to high energies via the stochastic acceleration process (e.g. Miller et al. (1997)). For electrons, except at very high energies, however, they do not resonate with Alfvén waves, therefore they interact with other waves, for example, fast mode and/or whistler waves (Miller et al. 1996).

Note that Drury et al. (1982) did not consider the effect of the energetic electrons on the shock. In a more refined and self-consistent analysis, the pressure of the energetic electrons needs to be taken into account and it will affect the shock width. This is similar to a modified shock structure caused by energetic cosmic rays as first examined by Axford, Leer & McKenzie (1982). Such a discussion, however, exceeds the scope of this work and we do not consider the back reaction of energetic electrons on the shock structure.

We assume the turbulence at a flare, as in the solar wind, is described by an inertial range joining to a dissipation range and the power density  $I(k)$  is given by,

$$I(k) = I(k_0) \left( \left( \frac{k}{k_b} \right)^{-\epsilon_i} H(k_b - k) + \left( \frac{k}{k_b} \right)^{-\epsilon_d} H(k - k_b) \right), \quad (4)$$

where  $\epsilon_i$  and  $\epsilon_d$  are the spectral indices in the inertial range and dissipation range, respectively. We assume  $\epsilon_d = 2.7$  (see below) and consider three cases for  $\epsilon_i$ :  $5/3$ ,  $1.5$  and  $1.0$ . The case of  $\epsilon_i = 5/3$  corresponds to a Kolmogorov cascading; the case of  $\epsilon_i = 1.5$  corresponds to a Iroshnikov-Kraichnan (IK) cascading, and the case of  $\epsilon_i = 1.0$  corresponds to a Bohm-like diffusion (see below). At very small  $k$ , the energy containing range sets in

and  $I(k)$  bent over. The normalization of  $I(k)$  is given by,

$$\int_{-\infty}^{+\infty} I(k) = \langle \delta B^2 \rangle. \quad (5)$$

For a wide range of electron energy, the resonating wavenumber  $k$  is in the dissipation range. In the solar wind, one finds a spectrum  $\sim k^{-2.7}$  to  $\sim k^{-3.0}$  in the dissipation range (Leamon et al. 1998, 1999; Chen et al. 2010; Howes et al. 2011; Alexandrova et al. 2012). Unlike the inertial range, the nature of the turbulence in the dissipation range is still under debate. Two possible scenarios include Landau damping of kinetic Alfvén waves e.g. (Leamon et al. 1999, 2000; Boldyrev and Perez 2012), or whistler waves e.g. (Stawicki et al. 2001; Krishan & Mahajan 2004; Galtier 2006). For KAWs,  $k_{\perp} \gg k_{\parallel}$ , electron-wave interaction is through the Landau resonance and KAWs can effectively heat electrons. Whistler waves have  $\omega_p < \omega < \Omega$  and electrons can interact with whistler waves through the cyclotron resonance. The resonance condition is,

$$\omega - k_{\parallel}v_{\parallel} = n\Omega \quad (6)$$

where  $\Omega = eB/(\gamma m_e)$  is the electron cyclotron frequency and  $\gamma$  is the Lorentz factor. For low frequency waves  $\omega < \Omega$ , the resonance condition (on taking  $n = 1$ ) yields

$$\mu v = \Omega/|k_{\parallel}| \quad (7)$$

where  $\mu$  is the pitch angle of the electron. Note from equation (6), one can see that when the energy of electron is high enough, it can also resonate with Alfvén waves. In this work, we assume the dissipation range turbulence is whistler-wave-like and electrons can resonate with the wave through the cyclotron resonance. As done in Gordon et al. (1999); Rice et al. (2003); Li et al. (2005), we further simplify the resonance condition by replacing  $k = \Omega/\mu v$  with  $k = \Omega/v$ , which corresponds to an extreme resonance broadening. The pitch angle diffusion coefficient  $D_{\mu\mu}$ , from the Quasi-linear Theory (QLT) (Jokipii 1966) is,

$$D_{\mu\mu} = \frac{1 - \mu^2}{|\mu|v} \frac{\Omega^2}{B_0^2} I(k = \Omega/\mu v) \quad (8)$$

The diffusion coefficient  $\kappa$  is related to  $D_{\mu\mu}$  through,

$$\kappa = \frac{v^2}{8} \int_{-1}^{+1} \frac{(1 - \mu^2)^2}{D_{\mu\mu}} = \frac{v^3 B_0^2}{16\Omega^2 I(k = \Omega/v)} \quad (9)$$

We make no attempts to estimate the turbulence level at the reconnection site in this work. Instead, we are more interested in the energy dependence of  $\kappa$ . From equation (9), we have

$$\kappa = \kappa_0 \frac{(p/p_0)^{3-\epsilon_{i,d}}}{\gamma} \quad (10)$$

where subscripts  $i$  or  $d$  denote whether electrons resonate with the inertial or the dissipation range of the turbulence. For electrons resonating with the dissipation range that have a  $\epsilon_d \sim 2.7$ , equation (10) suggests that  $\kappa$  has a very shallow dependence on electron momentum (energy). In comparison, for electrons resonating with the inertial range,  $\kappa$  increases quickly with particle momentum (energy). In Tsuneta & Naito (1998), the Bohm diffusion approximation was used, in which case  $\kappa \sim vR_l$ , where  $R_l$  is electron's gyroradius. This corresponds to an  $\epsilon_i = 1$ .

The fact that  $\kappa$  has a very shallow dependence on the electron's momentum in the dissipation range and a strong dependence in the inertial range is the key to understand the hardening of electron spectrum. In Figure 1 we plot  $\beta_s$  as defined in equation (3), where from equation (10), we have

$$\beta_s = \beta_0 \frac{(p/p_0)^{3-\epsilon_{i,d}}}{\gamma} \quad (11)$$

We set  $\beta_0 = 0.2$ . This value yields an electron spectral index at low energy to be  $\sim p^{-10}$ , comparable to flare observations.

Note, from equation (3),  $\beta_s$  also depends on the width of the shock. Simulations by Scholer & Burgess (2006) suggested that the shock width is of the order of ion inertial scale length  $\sim (c/\omega_{pi})$ . On the other hand, observations of the Earth's bow shock (at quasi-perpendicular configurations) showed that its ramp width is somewhat smaller than

182  $\sim (c/\omega_{pi})$  (Scudder et al. 1986; Balikhin et al. 1995; Newbury et al. 1998). In particular,  
 183 Newbury et al. (1998) found considerable fine structures of the order of  $\sim (c/\omega_{pe})$ .  
 184 Zank et al. (2001) suggested that these fine structures will help to circumvent the injection  
 185 problem for Anomalous cosmic rays. In a very recent study, using Clusters observation,  
 186 Schwartz et al. (2011) showed that at the Earth’s bow shock half of the temperature  
 187 occurred in about  $\sim 7c/\omega_{pe}$  or  $\sim (1/7)c/\omega_{pi}$ . The total width of the shock in Schwartz et al.  
 188 (2011), which is close to  $L_{diff}$  in our work, however, is another factor of  $\sim 6$  (see their  
 189 figure (3)). Therefore, in this work, we assume the shock width is given by the ion inertial  
 190 length scale  $L_{diff} \sim c/\omega_{pi}$ .

191 The break point  $p_b$  in Figure 1 is  $p_b \sim \gamma m_e \Omega / k_b$  with  $k_b$  the wave number separating  
 192 the inertial range and the dissipation range. The scale at which the inertial range transits  
 193 into the dissipation range is still a much debated issue. It has been argued that it could  
 194 be the thermal proton Larmor radius  $\sim \frac{\sqrt{k_B T / m_p}}{\Omega_p}$  (Leamon et al. 1998, 1999) or the  
 195 ion inertial length  $\sim \frac{V_A}{\Omega_p}$  with  $\Omega_p$  the proton cyclotron frequency (Leamon et al. 2000;  
 196 Smith et al. 2001). Consider a typical flare site (Miller et al. 1996; Mann et al. 2009) with  
 197 a temperature of  $T \sim 5$  MK, a magnetic field of  $B \sim 200$  Gauss and a density of  $n_e \sim 10^9$   
 198  $\text{cm}^{-3}$ , we find an Alfvén speed  $V_A \sim 1.38 * 10^4 \text{ km sec}^{-1}$ , a thermal proton speed  $v_{th} \sim 200$   
 199  $\text{km sec}^{-1}$ , a proton gyrofrequency  $\Omega_p = 1.91 * 10^6 \text{ Hz}$ . Consequently, the thermal ion  
 200 Larmor radius is  $\sim 0.10 \text{ m}$  and the ion inertial length is  $\sim 7.2 \text{ m}$ . If  $k_b$  is the reciprocal of  
 201 the thermal ion Larmor radius, then  $p_b \sim 0.64 \text{ MeV/c}$  and the corresponding kinetic energy  
 202 is  $0.31 \text{ MeV}$ . This is in good agreement to the observed continuum emission break locations  
 203  $\sim 300 \text{ keV}$ . On the other hand, if  $k_b$  is the reciprocal of the ion inertial length, then  $p_b \sim 39$   
 204  $\text{MeV/c}$ , much too high for the proposed scenario. Therefore our proposed scenario favors  
 205 the the suggestion of Leamon et al. (1998, 1999) that the dissipation range sets in at the  
 206 thermal ion Larmor radius scale. Comparing to the width of the shock, which is the ion  
 207 inertial length scale  $7.2 \text{ m}$ , the gyro-radius of an electron  $R_l = \gamma v / \Omega_e$  is  $0.1 (0.4) \text{ m}$  for a

kinetic energy of 300 keV (2 MeV).

Using a momentum dependent  $\beta_s$  as in equation (11), we numerically solve the steady-state transport equation. We set  $p_0$  to be 32 keV/c, which corresponds to an injection energy of 1 keV. We use the same shock profile as Drury et al. (1982), given by equation (1) and assume a compression ratio of 3.5 (thus a strong shock). Note that the outflow plasma speed at a reconnection site is  $\sim V_A$ . Therefore for a shock with a compression ratio of 3.5,  $u_1 - u_2$  in equation (3) is  $\sim 10^4$  km/s. We use  $\beta_0 = 0.2$ . Tsuneta & Naito (1998) have used the Bohm approximation for  $\kappa$ . With the Bohm approximation  $\kappa = \frac{1}{3}vR_l$  and the above values for a typical flare site, then a 300 keV electron will have  $\beta_s = 0.2$  and a 2 MeV electron will have  $\beta_s = 1.0$ , suggesting our choice of  $\beta_0 = 0.2$  is reasonable.

Figure 2 plots the steady state electron spectrum for three cases that have different inertial range turbulence spectrum: i): Kolmogorov-like; ii): IK-like; and iii): Bohm diffusion approximation. In each panel, the two dashed lines are power law fittings  $\sim (p/p_0)^{-\alpha}$ , with  $\alpha_1$  and  $\alpha_2$  the fitted spectral indices to the spectrum at the low and high energies respectively, and  $p_m$  the fitted break momentum. We set  $p_b$  to be  $13p_0 \sim 0.416$  MeV/c in the simulation, which corresponds to a  $E_b$  of 0.15 MeV. Note that  $p_m$  is larger than  $p_b = \gamma m_e \Omega / k_b$  by about a factor of  $\sim 2$ . Figure 2 is the most important result of this paper. It shows that diffusive shock acceleration at a finite-width termination shock in solar flares can naturally lead to a hardening of the accelerated electron spectrum.

### 3. Discussions and conclusions

Clearly, the hardening requires the following conditions to be met. First, the existence of a termination shock at flare site with a finite shock width  $L_{diff} \sim c/\omega_{pi}$ . Second, the

diffusion coefficient  $\kappa$  needs to be close to a constant at low energies and increases with electron energy at high energies. Third, it is necessary that  $\kappa < \Delta UL_{diff}$  at energies below the break and  $\kappa > \Delta UL_{diff}$  at energies above the break.

For any given flare, none of these conditions are necessarily satisfied.

Consider the first condition. While it is hard to identify a termination shock at a flare observationally, there are indirect clues of such shocks. For example, type II radio bursts without frequency drift has been used by Warmuth et al. (2009) to infer the existence of flare termination shocks. Further observational evidence of flare termination shock, and in particular its size, are welcomed.

For the second condition: if electrons resonate with the dissipation range of the turbulence through cyclotron resonance and that the dissipation range has a power spectrum  $I(k) \sim k^{-2.7}$ , then we find  $\kappa$  is indeed close to a constant at low energies and increases with electron energy at high energies. While in-situ solar wind observations do suggest such a  $\sim k^{-2.7}$  dissipation range, direct confirmation of such a  $k$  dependence in the flare site is impossible.

To satisfy the third condition will put a strong constraint on the turbulence level at the flare, which can vary much from one to another. Consequently, the hardening does not occur in all flares. For example, if for a given flare,  $\beta_s \sim 1$  instead of  $\beta_s \sim 0.2$  at lower energies, then there will be no hardenings, even if both conditions 1 and 2 are satisfied. Because a larger  $\beta_s$  implies a larger  $\kappa$ , therefore a less efficient acceleration, so one implication of our proposed scenario is the following: Events where the continuum emission extend to very high energies (efficient acceleration) likely show hardenings and have softer spectra at lower energies, and events where the continuum emissions do not extend to high energies (inefficient acceleration) likely have harder spectra at low energies than those events that extend to higher energies.

Another consequence of our proposal is the correlation between the low energy photon spectral index  $\gamma_1$  and the break momentum  $p_m$ . Consider two nearly identical flares A and B except that flare A has a larger  $k_b$  (i.e. the inertial range in flare A extends to a smaller scale). Then  $\beta_s$  at  $p < p_m$  for flare A is smaller. Therefore,  $p_m$  and  $\alpha_1$  are anti-correlated. Observations do show such a anti-correlation and this is discussed in details in Kong et al., (in preparation).

In summary, we offer an explanation for the observed continuum spectral hardening in solar flares that is based on DSA. To our knowledge, no previous works have addressed the hardening of emission spectrum explicitly. Further observational and theoretical studies along the proposed mechanism will be pursued in future works.

This work is supported in part by NSF grants ATM-0847719, AGS1135432, and NASA grants NNH07ZDA001N-HGI and NNX11AO64G at UAHuntsville and the 973 Program No. 2012CB825601 and NNSFC Grant Nos. 41274175 and 41028004 at SDUWH. XLK acknowledges financial support by the Shandong University Graduate Study Abroad Fund.

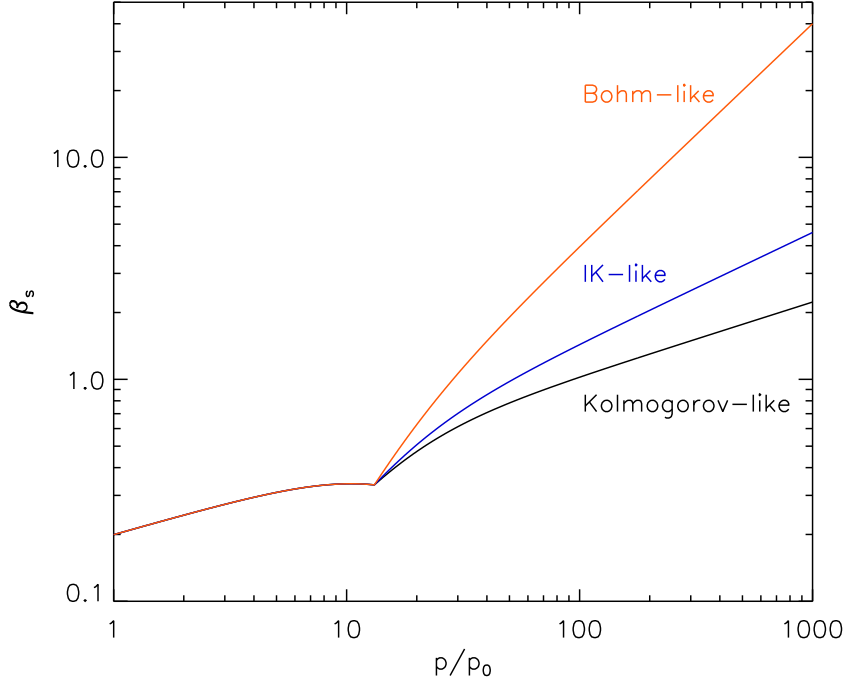


Fig. 1.—  $\beta_s$  as defined in equation (3). At low energies, electrons resonate with the dissipation range and  $\beta_s$  has a weak momentum dependence. Above  $p_b$ , electrons resonate with the inertial range and  $\beta_s$  quickly increases with momentum. Three cases for the inertial range are considered. These are, from top to bottom, Bohm-like, IK-like and Kolmogorov-like.



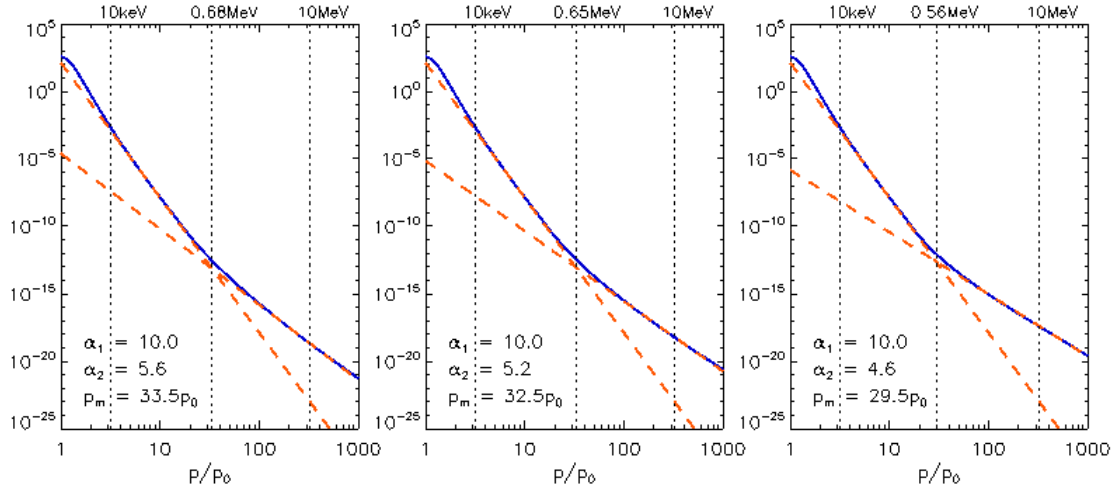


Fig. 2.— The electron spectrum for three cases: i: Kolmogorov-like inertial range; ii: IK-like inertial range; iii: Bohm diffusion Approximation.

## REFERENCES

- Alexandrova, O., Lacombe, C., Mangeney, A., Grappin, R., Maksimovi, M., 2012, ApJ, 760, 121
- Ackermann, M., Ajello, M., Allafort, A., et al. 2012, ApJ, 745, 144
- Balikhin, M. A., Krasnosselskikh, V., & Gedalin, M. 1995, Adv. Space Res., 15, 247
- Asai, A., Kiyohara, J., Takasaki, H., Narukage, N., Yokoyama, T., Masuda, S., Shimojo, M., and Nakajima, H., 2013, ApJ, 763, 87
- Axford, W.I., Leer, E., and McKenzie, J.F., 1982, A& A, 111, 317
- Boldyrev, S., and Perez, J. C., 2012, ApJL, 758, L44.
- Chen, C. H. K., Horbury, T. S., Schekochihin, A. A., et al. 2010, Phys. Rev. Lett., 104, 255002
- Drury, L. O’C., Axford, W. I., Summers, D. 1982, MNRAS, 198, 883
- Galtier, S. 2006, J. Plasmas Phys., 72, 721
- Guo, F., & Giacalone, J. 2012, ApJ, 753, 28
- Gordon, B. E., M. A. Lee, and E. Möbius, 1999, JGR, 104, 28263-28277.
- Howes, G. G., Tenbarger, J. M., & Dorland, W. 2011, Phys. Plasmas, 18, 102305
- Jokipii, J., 1966, ApJ, 146, 480.
- Kawate, T., Nishizuka, N., Oi, A.; Ohyama, M., and Nakajima, H., 2012, ApJ, 747, 131
- Kontar, E. P., Emslie, A. G., Massone, A. M., et al. 2007, ApJ, 670, 857
- Krishan, V. & Mahajan, S. M. 2004, JGR, 109, A11105

- 290 Lee, M. A. 1983, JGR, 88, 6109
- 291 Li, G., Zank, G. P., Rice, W. K. M. 2005, JGR, 110,A06104
- 292 Lin, R. P., Dennis, B. R., Hurford, G. J., et al. 2002, Sol. Phys., 210, 3
- 293 Leamon, R. J., Smith, C. W., Ness, N. F., Matthaeus, W. H., Wong, H. K. 1998, JGR, 103,  
294 4775
- 295 Leamon, R. J., Smith, C. W., Ness, N. F., Wong, H. K. 1999, JGR, 104, 22331
- 296 Leamon, R. J., Matthaeus, W. H., Smith, C. W., et al. 2000, ApJ, 537, 1054
- 297 Mann, G., Warmuth, A., Aurass, H. 2009, A&A, 494, 669
- 298 Marschhauser, H., Rieger, E., Kanbach, G. 1994, AIP Conference Proceedings, 294, 171
- 299 Melrose, D. B., & Brown, J. C., 1976, MNRAS, 176, 15
- 300 Miller, J. A., Larosa, T. N., Moore, R. L., 1996, ApJ, 461, 445
- 301 Miller, J. A., Cargill, P. J., Emslie, A. G., et al., 1997, JGR, 102, 14631
- 302 Moses, D., Droge, W., Meyer, P., Evenson, P., 1989, ApJ, 346, 523.
- 303 Newbury, J. T., Russell, C. T., and Gedalin, M., 1998, J. Geophys. Res., 103, 29581
- 304 Park, B. T., Petrosian, V., Schwartz, R. A. 1997, ApJ, 489, 358
- 305 Petrosian, V., McTiernan, J. M., Marschhauser, H. 1994, ApJ, 434, 747
- 306 Ramaty, R., Kozlovsky, B., Lingenfelter, R. E. 1975, Space Sci. Rev., 18, 341
- 307 Rieger, E., & Marschhauser, H. 1990, in Proc. of the Third Max 91 Workshop, ed. R. M.  
308 Wingler & A. L. Kiplinger, 68

- 309 Rice, W. K. M., Zank, G. P., Li, G. 2003, JGR, 108, 1082
- 310 Scholer, M., & Burgess, D. 2006, Phys. Plasmas, 13, 062101
- 311 Schwartz, S. J., Henley, E., Mitchell, J., Krasnoselskikh, V. 2011, PRL, 107, 215002
- 312 Scudder, J. D., et al. 1986, J. Geophys. Res., 91, 1053
- 313 Silva, A. V. R., Wang, H., & Gary, D. E. 2000, ApJ, 545, 1116
- 314 Smith, C. W., Mullan, D. J., Ness, N. F., Skoug, R. M., Steinberg, J. 2001, JGR, 106, 18625
- 315 Stawicki, O., Gary, S. P., Li, H. 2001, JGR, 106, 8273
- 316 Suri, A. N., Chupp, E. L., Forrest, D. J., Reppin, C. 1975, Sol. Phys., 43, 415
- 317 Tsuneta, S. & Naito, T. 1998, ApJL, 495, L67
- 318 Vestrand, W. T. 1988, Sol. Phys., 118, 95
- 319 Vestrand, W. T., Share, G. H., Murphy, R. J., et al. 1999, ApJS, 120, 409
- 320 Warmuth, A., Mann, G., Aurass, H. 2009, A&A, 494, 677
- 321 White, S. M., Benz, A. O., Christe, S., Fárník, F., Kundu, M. R., Mann, G., Ning, Z.,  
322 Raulin, J.-P., Silva-Válio, A.V.R., Saint-Hilaire, P., Vilmer, N., Warmuth, A., 2011,  
323 Space Sci. Rev., 159, 225, doi: 10.1007/s11214-010-9708-1
- 324 Yoshimori, M., Watanabe, H., Nitta, N. 1985, JPSJ, 54, 4462
- 325 Zharkova, V. V., Arzner, K., Benz, A. O., et al. 2011, Space Sci. Rev., 159, 357
- 326 Zank, G. P., Rice, W. K. M., le Roux, J. A. and Matthaeus, W. H., 2001, ApJ, 556, 494